# Relativistic Positron-Electron Bremsstrahlung at Wide Angles: A Numerical Calculation*

STANLEY M. SWANSON
*Institute of Theoretical Physics, Department of Physics, Stanford University, Stanford, California*
(Received 29 September 1966)

The bremsstrahlung spectrum for the process $e^+ + e^- \rightarrow e^+ + e^- + \gamma$ has been evaluated at photon-emission angles of roughly 30° to 120° from the incident particles in the c.m. system. The phase-space integrals of the exact, lowest-order differential cross section were evaluated numerically. A computer program was used to reduce the Dirac traces to invariants and to further simplify them until reasonably compact expressions were obtained. Numerical results for selected photon angles and energies are given for 15-BeV positrons incident upon electrons at rest in the laboratory and for 600- and 4000-MeV positrons in the c.m. system (colliding-beam experiments). It was found that certain relativistic approximations to the spectrum, which are valid for forward angles, are still fairly good at wide angles; an empirical modification to such an approximation is given which provides a useful interpolation formula for the wide-angle region.

## I. INTRODUCTION

THE bremsstrahlung produced in positron-electron collisions is of interest for the estimation of background in various processes: for positron annihilation in flight to produce a gamma ray beam[1] and for colliding beam experiments. This work was originally undertaken as part of a calculation of the photon spectrum in the process $e^+ + e^- \rightarrow 2\gamma$ which has been suggested as a means of producing a high energy, nearly monochromatic photon source with the Stanford two-mile linear accelerator.[2] The complete spectrum requires calculation of two and three quantum annihilation, radiative corrections, and bremsstrahlung from the nucleus used to localize the target electrons.[3] Such an analysis indicates that the optimum photon production angles are near 90° in the c.m. system (but only 0.008 rad in the laboratory for 15-BeV positrons). The results of this work are also of use in the analysis of wide angle $e^+ - e^-$ scattering experiments in the c.m. system which have been proposed as tests of quantum electrodynamics at small distances.

For relativistic particles at forward angles, very satisfactory approximations to the bremsstrahlung spectrum can be made by analytically integrating only two of the eight lowest-order Feynman graphs, but it was not apparent that this would work at wide angles. Instead, we did numerical phase-space integrals of the exact, lowest-order differential cross section. Although the traces involved in the square of the matrix element $(\Sigma|M|^2)$ for this process have been evaluated before, once by Votruba[4] for pair production in the field of an electron and again by Hodes[5] for electron-electron bremsstrahlung, the application of the substitution rule to such long expressions is tedious and subject to error. Hence we started anew, using a computer program to reduce the Dirac traces algebraically to invariants and eventually to further simplify them.

The results of the numerical integration over the phase space of the unobserved $e^+ - e^-$ pair show that the small angle formulas are remarkably good even at $90°_{\text{c.m.}}$ and that a simple empirical modification will give a 1 to 5% numerical fit to the exact spectrum except near the high-energy end where other diagrams introduce a peak. Some numerical results are given to illustrate the accuracy of this and other approximation schemes; more extensive cross-section tables are available elsewhere.[6] The interest of this paper lies also in indicating some of the problems encountered in doing the numerical phase-space integrals in the ultrarelativistic region, so the technical details and some general remarks about the use of computer programs in quantum electrodynamics are given in the Appendix.

## II. PERTURBATION CALCULATION

In lowest order ($\alpha^3$), the eight Feynman diagrams of Fig. 1 define the matrix element of positron-electron bremsstrahlung. We denote the initial electron and positron four-momenta by $p_1$ and $p_2$, respectively, the final photon by $k$, and the final electron and positron by $p_3$ and $p_4$, respectively. There are three distinct types of traces in $\Sigma|M|^2$; once these are reduced to dot products, all other traces may be obtained by substitutions among the invariants.

Before specifying these traces we introduce a shorthand notation. Let the particle propagators and projection operators be $S(q)=(q\cdot\gamma-m)^{-1}$ and $\Lambda(\pm p_i)=(m\pm p_i\cdot\gamma)/2m$, and the four possible internal electron momenta: $q_1=p_1-k$, $q_2=k-p_2$, $q_3=k+p_3$, and

* Work supported in part by the U. S. Air Force Office of Scientific Research under Contract No. AF 49(638)-1389 and in part by the U. S. Atomic Energy Commission.

[1] A preliminary version of some of the numerical results of this paper has appeared: Y. S. Tsai, S. M. Swanson, and C. K. Iddings, in *Proceedings of the International Symposium on Electron and Photon Interactions at High Energies* (Deutsche Physicalische Gesellschaft e.V., Hamburg, 1966), Vol. II, p. 380.

[2] J. Ballam and Z. G. T. Guiragossian, in *Proceedings of the Twelfth Annual International Conference on High-Energy Physics, Dubna, 1964* (Atomizdat, Moscow, 1965).

[3] Y. S. Tsai, Phys. Rev. **137**, B730 (1965).

[4] V. Votruba, Bull. Intern. Acad. Tcheque Sci. **49**, 19 (1948); Phys. Rev. **73**, 1468 (1948).

[5] I. Hodes, Ph.D. thesis, University of Chicago, 1953 (unpublished).

[6] A. Dufner, S. Swanson, Y. Tsai, SLAC Report 67, Stanford Linear Accelerator Center, Stanford, California, 1966 (unpublished).

TABLE I. The computer-generated traces from Eqs. (2–4). Note that twice the interference traces ($2B$,$2C$) are given and that the $m^{-4}$ from the particle projection operators has been factored out in the definitions of $A$, $B$, and $C$. We use the abbreviated symbols: $K_1=k\cdot p_1$, $K_2=k\cdot p_2$, $K_3=k\cdot p_3$, $K_4=k\cdot p_4$, $Q=m^2-p_2\cdot p_4$, $Q'=m^2-p_1\cdot p_3$, $S=p_1\cdot p_2$, $U=\frac{1}{2}l^2$, $V=p_3\cdot p_4$.

$$A=-\tfrac{1}{2}m^2(1/K_1^2+1/K_3^2)+1/K_1-1/K_3-(S+V+Q+m^2)/K_1K_3-m^2Q^{-2}(S/K_3-V/K_1-1)^2$$
$$-Q^{-1}\{m^2(1/K_3-1/K_1)[m^2(1/K_3-1/K_1)+1+S/K_3-V/K_1]+V/K_3-S/K_1$$
$$+(S^2+V^2)/K_1K_3+\tfrac{1}{2}(K_3/K_1+K_1/K_3)(1+m^2/Q)\}$$

$$2B=(1/QQ')\{\tfrac{1}{4}(1/K_1K_2+1/K_3K_4)(S+V)[(S+V)(S+V+Q+Q')+Q^2+Q'^2+2m^2(Q+Q')]$$
$$-\tfrac{1}{8}(1/K_1K_4+1/K_2K_3)(S+V+Q+Q')[(S+V+Q+Q')^2+2S^2+2V^2+4m^2(Q+Q')]$$
$$+\tfrac{1}{2}(S+V+Q+Q')+\tfrac{1}{8}(K_1/K_4+K_4/K_1+K_2/K_3+K_3/K_2)(S+V-Q-Q')$$
$$-\tfrac{1}{2}m^2[(Q+Q'+2S+2V)(1/K_3+1/K_4-1/K_1-1/K_2)$$
$$+(K_2+K_4)(1/K_1+1/K_3)+(K_1+K_3)(1/K_2+1/K_4)]\}$$

$$2C=(1/QU)\{[(Q+U)^2-m^4][-m^2/K_1^2+2/K_2-2/K_3+V/K_1K_2-(Q-m^2)/K_1K_3$$
$$+(m^2-Q-U-3K_1)/K_2K_3]+\tfrac{1}{2}m^2[(3Q+3U-K_4)/K_1-3]$$
$$+\tfrac{1}{2}(1/K_2-1/K_3)[(Q+U)(5K_1+3K_4)+K_1(2K_1+K_4)+K_4(K_4+m^2-2m^2(Q+U+m^2)/K_1)]$$
$$+\tfrac{1}{2}(U/K_2-Q/K_3)[(2Q+2U-m^2)(1+K_4/K_1)+K_1+K_4^2/K_1]$$
$$-(K_1/K_2K_3)[K_1(3Q+3U+K_1)-3m^2(Q+U)/2]\}$$

$q_4=-k-p_4$. Then define the symbol

$$[i\mu j]=[e\cdot\gamma S(q_i)\gamma_\mu+\gamma_\mu S(q_j)e\cdot\gamma], \quad (1)$$

where $e$ is the polarization vector of the external photon. When the photon polarization sum is taken, $\cdots e\cdot\gamma\cdots e\cdot\gamma\cdots$ is replaced by $\cdots(-\gamma_\lambda)\cdots(\gamma_\lambda)\cdots$. Denote by $A$, $B$, and $C$, the three parts of $\Sigma|M|^2$ arising from the two graphs of Fig. 1(a) combined with those of Figs. 1(a), 1(b), and 1(c), respectively:

$$m^{-4}A=(p_2-p_4)^{-4}\,\mathrm{tr}\{\Lambda(p_3)[3\mu1]\Lambda(p_1)[1\nu3]\}$$
$$\times\mathrm{tr}\{\Lambda(-p_2)\gamma_\mu\Lambda(-p_4)\gamma_\nu\}, \quad (2)$$

$$m^{-4}B=(p_2-p_4)^{-2}(p_1-p_3)^{-2}$$
$$\times\mathrm{tr}\{\Lambda(p_3)[3\mu1]\Lambda(p_1)\gamma_\nu\}$$
$$\times\mathrm{tr}\{\Lambda(-p_2)\gamma_\mu\Lambda(-p_4)[4\nu2]\}, \quad (3)$$

$$m^{-4}C=-(p_2-p_4)^{-2}(p_3+p_4)^{-2}\,\mathrm{tr}\{\Lambda(p_3)[3\mu1]$$
$$\times\Lambda(p_1)[1\nu2]\Lambda(-p_2)\gamma_\mu\Lambda(-p_4)\gamma_\nu\}. \quad (4)$$

With the following indicated substitutions, these three traces suffice to evaluate $\Sigma|M|^2$ (to verify this requires the fact that the trace of a string of Dirac matrices is equal to the trace of the string written in reverse order):

$$m^4\sum_{\text{pol., spins}}|M|^2=A+A(p_1\leftrightarrow-p_4,\ p_2\leftrightarrow-p_3)$$
$$+A(p_2\leftrightarrow-p_3)+A(p_1\leftrightarrow-p_4)$$
$$+2B+2B(p_1\leftrightarrow-p_4)+2C+2C(p_1\leftrightarrow-p_4)$$
$$+2C(p_1\leftrightarrow p_3,\ p_2\leftrightarrow p_4,\ k\leftrightarrow-k)$$
$$+2C(p_1\leftrightarrow-p_2,\ p_3\leftrightarrow-p_4,\ k\leftrightarrow-k). \quad (5)$$

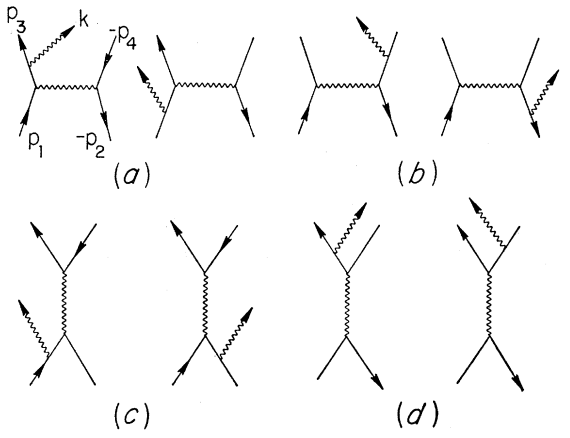


FIG. 1. The Feynman diagrams for $e^+-e^-$ bremsstrahlung, paired according to common photon propagators.

The actual reduction of the three basic traces to dot products was done on an IBM 7090 computer by a machine language program written to do Dirac algebra symbolically.[7] With the conditions $p_i^2=m^2$ and $k^2=0$ imposed, the computation time was about 5 sec per trace. In this case, $A$ had 48 terms, while $B$ and $C$ had about 120 terms apiece, resulting in almost 900 terms for the full expression of Eq. (5). Each term is a product of three dot products, divided by four propagator denominators. Using other identities, it was possible to combine or cancel (by hand) about 30% of the terms. The end result in Table I was achieved after the algebra program was rewritten to allow substitutions of linear combinations of invariants for individual dot products.

A cross section is obtained by multiplying $\Sigma|M|^2$ by the phase space factor and dividing by the flux; to get the photon spectrum, we must integrate over the possible momenta of the unobserved final particles.

$$d\sigma=\frac{\alpha r_0^2m^2\omega d\omega d\Omega_k}{8\pi^2((p_1\cdot p_2)^2-m^4)^{1/2}}$$
$$\times\int_0^{2\pi}d\phi\int_{-1}^{1}d(\cos\theta)\beta m^4\Sigma|M|^2. \quad (6)$$

[7] A description of this program has been given in S. M. Swanson, Institute of Theoretical Physics, Stanford University. Report No. ITP-120 (unpublished).

TABLE II. Dot products and related kinematical quantities as functions of $m$, $\omega$, $E$, $\chi$, $\theta$, $\phi$. In the laboratory frame, the incident positron ($p_2$) has energy $E$ and the incident electron ($p_1$) is at rest with energy $m$, whereas in the center-of-mass frame, both incident particles have energy $E$. In either frame, a final photon of energy $\omega$ is emitted at an angle $\chi$ from $\mathbf{p}_2$; $\omega_{\max}$ is the maximum possible photon energy. The special direction of the final positron ($p_4$) is given by the angles $\theta$, $\phi$ in the special frame. The quantities $t$, $P$, $\beta$ are auxiliary variables, introduced only for convenience.

$$P=(E^2-m^2)^{1/2} \qquad t_\mu=(p_3+p_4)_\mu \qquad \beta=(1-4m^2t^{-2})^{1/2}$$

Laboratory frame quantities:

$$p_1\cdot p_2=mE \qquad k\cdot p_1=m\omega \qquad k\cdot p_2=\omega(E-P\cos\chi)$$
$$\omega_{\max}=m(E-m)/(m+E-P\cos\chi)$$

Center-of-mass system quantities:

$$p_1\cdot p_2=E^2+P^2 \qquad k\cdot p_1=\omega(E+P\cos\chi) \qquad k\cdot p_2=\omega(E-P\cos\chi)$$
$$\omega_{\max}=E-(m^2/E)$$

Other dot products:

$$t\cdot k=k\cdot p_1+k\cdot p_2 \qquad t^2=2(m^2+p_1\cdot p_2-t\cdot k)$$
$$p_3\cdot p_4=\tfrac{1}{2}t^2-m^2 \qquad t\cdot p_2=m^2+p_1\cdot p_2-k\cdot p_2$$
$$k\cdot p_3=\tfrac{1}{2}t\cdot k(1+\beta\cos\theta) \qquad k\cdot p_4=t\cdot k-k\cdot p_3$$
$$p_2\cdot p_3=\tfrac{1}{2}t\cdot p_2+\tfrac{1}{2}\beta\cos\theta(t\cdot p_2-k\cdot p_2(t^2)(t\cdot k)^{-1})+\tfrac{1}{2}\beta\sin\theta\cos\phi(t\cdot k)^{-1}[t^2(t^2+2t\cdot k)k\cdot p_1(k\cdot p_2)-m^2t^2(t\cdot k)^2]^{1/2}$$
$$p_1\cdot p_3=\tfrac{1}{2}t^2+k\cdot p_3-p_2\cdot p_3$$
$$p_2\cdot p_4=p_1\cdot p_3+k\cdot p_1-k\cdot p_3$$
$$p_1\cdot p_4=\tfrac{1}{2}t^2+k\cdot p_4-p_2\cdot p_4$$

Note that the remaining phase-space of the photon, $\omega d\omega d\Omega_k$, is separately invariant and can be evaluated in that frame in which the spectrum is desired. Since the kinematical constraints on $p_3$ and $p_4$ take a complicated form in the laboratory frame, we have chosen to do this integration in the frame where the 3-vector part of $p_3+p_4$ is zero. We shall call this the "special frame." In the special frame, the direction of $\mathbf{p}_4$ is arbitrary, and the energies of the final electron and positron are equal and are determined once the photon energy and angle and the incident energies are fixed in some system. We have chosen the $z$ axis of the special frame to be along $\mathbf{k}$ and $\theta$ to be the angle between $\mathbf{k}$ and $\mathbf{p}_4$ (see Fig. 2), so that $d\Omega_4=d(\cos\theta)d\phi$. A straightforward application of Lorentz kinematics gives the dot products in terms of $m$, $\theta$, $\phi$, and the initial system quantities $E$, $\omega$, $\chi$ (see Table II). Some numerical integrals of the exact expression for $\Sigma|M|^2$ [Eq. (5)] are shown in Table III in column 3 and the technical details of the integration are given in the Appendix. The accuracy of the numerical integrals is believed to be better than 1% except in a few low-energy ($y\ll1$), small-angle cases marked by an asterisk which are probably 3 to 6% lower than the correct values.

## III. DISCUSSION

The numerical calculation of the exact cross section values in Table III is somewhat complicated and time consuming, so it was deemed desirable to develop fairly accurate approximate formulas for interpolation and extrapolation to nearby points in the spectrum. Two approximations were investigated: The first depends on the dominance of the propagators in determining the behavior of the integrand and the second depends on an empirical modification of a small-angle formula.

Perhaps the most striking feature of $\Sigma|M|^2$ in the ultrarelativistic region is an extreme peakedness in directions near the minima of the quantities $k\cdot p_3$, $k\cdot p_4$, $m^2-p_2\cdot p_4$, and $m^2-p_1\cdot p_3$ which appear as propagator denominators. This corresponds to the tendency of electromagnetic processes to peak in the forward direction at these energies; most of the radiation occurs when one of the final particles is only slightly deviated from its initial motion, or comes away near the photon direction. These peaks have made the numerical integration difficult, but have suggested an effective approximation motivated by the Schiff approximation to the Bethe-Heitler cross section for electron bremsstrahlung in the Coulomb field of a nucleus.[8]

The approximation consists of evaluating all the invariants, except the one whose minimum produces the peak, at the peak center and integrating the resulting function of the single invariant. In addition, we make a small-energy approximation, with

$$y=t\cdot k/(\tfrac{1}{2}t^2+t\cdot k)\approx\omega/\omega_{\max}(\text{lab})\approx\omega/E(\text{c.m.})\ll1. \quad (7)$$

Consider the peak in $q^2=m^2-p_2\cdot p_4$ for the trace $A$. At $|q^2|_{\min}$, we have $k\cdot p_3\approx k\cdot p_1(1+k\cdot p_2/t\cdot p_2)$, which

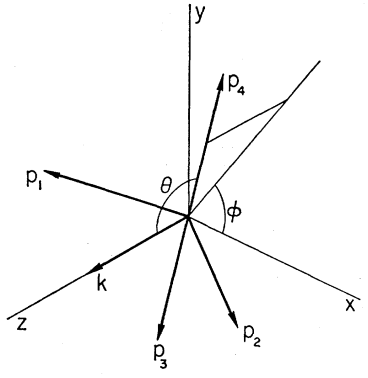


FIG. 2. The coordinate system in the special frame; $\mathbf{p}_1$, $\mathbf{p}_2$, and $\mathbf{k}$ lie in the $x$-$z$ plane.

[8] L. I. Schiff, Phys. Rev. **87**, 750 (1952).

TABLE III. Cross sections for the photon spectrum $(d^2\sigma/d\omega d\Omega_k)$ in the process $e^+ + e^- \rightarrow e^+ + e^- + \gamma$ for selected photon angles and energies in three initial systems. The photon is emitted at an angle $\chi$ with respect to the initial positron direction $\mathbf{p}_2$ and has a fraction $y$ of its maximum possible energy $\omega_{max}$. Column 3 contains the numerical integrals of the exact $\Sigma|M|^2$ [Eq. (5)]. The other five columns are various approximations which are more fully explained in the text. Column 4 omits the contributions of the annihilation graphs of Figs. 1(c) and 1(d), while column 5 omits both the annihilation graphs and the interference term between the graphs of Figs. 1(a) and 1(b). Columns 6 and 7 are, respectively, small- and wide-angle approximations to column 5. Column 8 is the result of an empirical modification to column 6 to fit the exact values [Eq. (12)]. The numerical integrals in columns 3 and 4 are believed to be accurate to better than 1% except in a few low $y$, small-angle cases (marked by an asterisk) which are probably about 5% low.

Cross sections in mb/BeV sr for a 15-BeV positron incident upon an electron at rest in the laboratory. The two low $y$ points at each angle correspond to 100- and 20-MeV photons. Some auxiliary parameters for these initial conditions are given in Table IV.

| $\chi$ (rad) | $y$ | Exact | $\int ABA$ | $\int AA$ | Small | Wide | Fudge |
|---|---|---|---|---|---|---|---|
| 0.002 | 0.8 | 38.66 | 39.6 | 38.47 | 43.82 | 45.99 | 40.57 |
| | 0.4 | 128.6 | 131.1 | 129.3 | 134.4 | 170.4 | 126.7 |
| | 0.1 | 805.0 | 819.0 | 815.8 | 834.6 | 1026.0 | 796.8 |
| | 0.00706 | 15380.0 | 15600.0 | 15620.0 | 15900.0 | 18670.0 | 15240.0 |
| | 0.00141 | 83930.0* | 83300.0* | 87180.0 | 88590.0 | 102500.0 | 84940.0 |
| 0.003 | 0.8 | 7.847 | 8.09 | 7.603 | 9.39 | 9.040 | 8.413 |
| | 0.4 | 26.52 | 27.4 | 26.67 | 28.81 | 33.51 | 26.48 |
| | 0.1 | 169.3 | 173.0 | 170.4 | 178.9 | 203.4 | 167.5 |
| | 0.00756 | 3015.0 | 3095.0 | 3050.0 | 3170.0 | 3489.0 | 2986.0 |
| | 0.00151 | 16710.0 | 17050.0 | 17080.0 | 17680.0 | 19270.0 | 16660.0 |
| 0.005 | 0.8 | 1.323 | 1.36 | 1.187 | 1.639 | 1.348 | 1.404 |
| | 0.4 | 4.448 | 4.57 | 4.274 | 5.029 | 5.019 | 4.468 |
| | 0.1 | 28.28 | 29.18 | 27.90 | 31.22 | 31.05 | 28.48 |
| | 0.00911 | 415.4 | 427.0 | 412.4 | 451.8 | 445.3 | 415.4 |
| | 0.00182 | 2336.0 | 2390.0 | 2328.0 | 2526.0 | 2491.0 | 2324.0 |
| 0.008 | 0.8 | 0.4902 | 0.489 | 0.4028 | 0.5886 | 0.4264 | 0.4933 |
| | 0.4 | 1.573 | 1.59 | 1.435 | 1.806 | 1.602 | 1.579 |
| | 0.1 | 10.03 | 10.14 | 9.484 | 11.21 | 10.09 | 10.10 |
| | 0.0129 | 101.9 | 102.1 | 96.69 | 111.2 | 100.8 | 101.1 |
| | 0.00259 | 571.4 | 578.1 | 552.0 | 625.3 | 572.2 | 568.9 |
| 0.012 | 0.8 | 0.4413 | 0.449 | 0.3836 | 0.5421 | 0.4257 | 0.4601 |
| | 0.4 | 1.461 | 1.50 | 1.379 | 1.664 | 1.590 | 1.468 |
| | 0.1 | 9.337 | 9.57 | 9.047 | 10.33 | 9.900 | 9.374 |
| | 0.0208 | 55.64 | 57.2 | 54.55 | 61.17 | 58.41 | 55.92 |
| | 0.00415 | 318.4 | 327.0 | 313.9 | 347.5 | 332.8 | 318.2 |
| | | Cross sections in nb/BeV sr for 600-MeV positrons in the center-of-mass system. | | | | | |
| 0.524 | 0.8 | 188.2 | 194.0 | 189.6 | 218.2 | 213.9 | 200.5 |
| | 0.1 | 3608.0 | 3681.0 | 3670.0 | 3779.0 | 4337.0 | 3592.0 |
| 1.571 | 0.8 | 5.995 | 6.071 | 5.309 | 7.796 | 5.595 | 6.531 |
| | 0.1 | 117.2 | 119.0 | 112.8 | 135.0 | 118.7 | 121.6 |
| | | Cross sections in nb/BeV sr for 4-BeV positrons in the center-of-mass system. | | | | | |
| 0.524 | 0.8 | 0.8119 | 0.8382 | 0.8230 | 0.9443 | 0.9058 | 0.8679 |
| | 0.1 | 14.45* | 14.77* | 15.18 | 15.65 | 17.50 | 14.87 |
| 1.571 | 0.8 | 0.02502 | 0.02550 | 0.02294 | 0.03373 | 0.02413 | 0.02826 |
| | 0.1 | 0.4751 | 0.4827 | 0.4647 | 0.5589 | 0.4861 | 0.5036 |

introduces considerable simplification for small $y$. Under these conditions, the peak shape is

$$A \propto q^{-4}(q^2+(1-k\cdot p_2/t\cdot p_2)|q^2|_{\min}). \quad (8)$$

Instead of the $q^{-4}$ behavior of potential scattering, there has been a cancellation in the numerator to produce a $q^{-2}$ peak with still further cancellation at the center which introduces a "crater" of several orders of magnitude.[9] Such cancellation may be understood qualitatively on the basis of helicity conservation in the electron-photon interaction.[10] Doing the same thing for $k\cdot p_3$, and by symmetrizing the formula to include the other two propagators, we obtain

$$\frac{d^2\sigma}{d\omega d\Omega} \approx \frac{\alpha r_0^2 m^2 \omega}{4\pi (k\cdot p_1)^2}\left\{(2-y)^2 \ln\left[\frac{t^2}{m^2}\left(\frac{t\cdot p_2}{k\cdot p_1}\right)^2\right] - (8-6y)\left(\frac{t\cdot p_2}{p_1\cdot p_2}\right) + \left[1+\left(\frac{k\cdot p_2}{t\cdot k}\right)^2\right](2-y)\ln\frac{t^2}{m^2}\right\} + \{p_1 \leftrightarrow p_2\}. \quad (9)$$

[9] The actual cancellation was somewhat larger than that indicated by Eq. (8). For example, in the case $E_{lab}=15$ BeV, $\chi_{lab}=0.008$, $y=0.1$, the photon peak $A \propto q^{-4}(q^2+0.99|q^2|_{\min})$.

[10] At least in the case of the electron propagators $(k\cdot p_3, k\cdot p_4)$, we can argue: If the electron mass is neglected, the interaction of electrons and photons conserves fermion helicity. Photon emission in the same direction as the fermion 3-momentum is forbidden by helicity conservation. With fermions of nonzero rest mass, emission in this direction is no longer strictly forbidden, but at high energies it is much less probable than emission at nearby angles, where the photon has a small transverse momentum.

From the numerical values of Eq. (9) in column 7 of Table III, we see that the approximation is remarkably good as $y$ approaches 1 and that the major contribution to the cross section comes from only a few of the traces in $\Sigma|M|^2$. Strictly speaking, this approximation does not include interference terms from trace $B$, so that the close agreement with the exact values at $90°_{\text{c.m.}}$ indicates an overestimate. The overestimate worsens at small angles since the peaks are treated independently, whereas in fact the electron and photon propagator peaks coalesce.

In small-angle, small-momentum transfer bremsstrahlung, the process is dominated by radiation from the incident lepton. This is described by neglecting all but the two graphs of Fig. 1(b), leading to a trace of type $A$. Theoretical arguments that the contributions from other terms should be less than a few percent for $\chi_{\text{c.m.}}<0.1$ have been given by Altarelli and Buccella.[11] The integrals involved for the trace $A$ are elementary but tedious and there is a large cancelation between the integrals coming from terms containing $q^{-4}$. What is surprising is that the result, when symmetrized to include the graphs of Fig. 1(a) but not the interference term (see Table III, column 5), should come so close to the exact result at all angles. The effect of including the interference term (trace $B$) in a numerical integration is given in column 4 of Table III, showing that the annihilation graphs [Figs. 1(c), 1(d)] can be neglected for $y\leqq 0.8$ to an accuracy of a few percent. However, for $\omega$ very close to $\omega_{\max}$, the graphs of Fig. 1(c) dominate the cross section; this will be discussed below.

At forward angles, the analytic integral of the trace $A$ [Eq. (2)] can be considerably simplified. This has been done by Altarelli and Buccella[11]:

$$\frac{d^2\sigma}{d\omega d\Omega}\approx\frac{\alpha r_0^2 m^2\omega}{2\pi(k\cdot p_2)^2}\left\{\left[2[1+(1-y)^2]+8(1-y)\left(\frac{1-\zeta}{\zeta^2}\right)\right]\ln\frac{t^2}{m^2y}-(2-y)^2-16(1-y)\left(\frac{1-\zeta}{\zeta^2}\right)\right\} \quad (10)$$

and by Tsai[1]:

$$\frac{d^2\sigma}{d\omega d\Omega}\approx\frac{\alpha r_0^2 m^2\omega}{2\pi(k\cdot p_2)^2}\left\{\left[2[1+(1-y)^2]+8(1-y)\left(\frac{1-\zeta}{\zeta^2}\right)\right]\ln\frac{t^2}{m^2y}-(2-y)^2+(1-y)\left(1-\frac{10}{\zeta}+\frac{42}{\zeta^2}-\frac{20}{\zeta^3}\right)\right\}. \quad (11)$$

[11] G. Altarelli and F. Buccella, Nuovo Cimento 34, 1337 (1964).

The parameter $\zeta=k\cdot p_2(t^2+2t\cdot k)/m^2t\cdot k$ approaches 1 as $y$ and $\chi$ both approach 0. The discrepancy between the two formulas is as high as 7% at small angles; a numerical comparison with the unapproximated integral indicates that Eq. (10) is probably correct. The formula of Altarelli and Buccella is identical to Schiff's approximation when the effect of screening is omitted in the latter.[12] At wide angles, these formulas must be symmetrized ($p_1\leftrightarrow p_2$) to include the backward angle peak and both formulas give essentially identical values (see Table III, column 6). They give an overestimate near $90°_{\text{c.m.}}$ when compared to column 5, since negative contributions from terms in $(k\cdot p_4)^{-1}$ and $(m^2-p_1\cdot p_3)^{-1}$ have been ignored in the small-angle approximation. The neglected terms and the contribution of the interference trace proved difficult to estimate for large $y$; it was felt better to devise a fudge factor to apply to the symmetrized Eq. (10) in order to reproduce the exact integral, rather than to take a selection of the neglected terms from column 5. One possible form is

$$\frac{d^2\sigma}{d\omega d\Omega}\approx[1-0.09(1+y)\sin\chi_{\text{c.m.}}]\times\{\text{Eq. (10), symmetrized } p_1\leftrightarrow p_2\}. \quad (12)$$

The agreement between the values of this numerical fit and the exact integral (compare columns 8 and 3 of the first part of Table III) is typical of that obtained for laboratory energies between 2 and 30 BeV; the worse fit in the second and third parts of Table III suggests that the numerical coefficient of $\sin\chi_{\text{c.m.}}$ is energy-dependent. (See also Table IV.)

Near the tip of the bremsstrahlung spectrum (for $y>0.999$), the process is dominated by the annihilation graphs of Fig. 1(c) whose photon propagator $t^2$ is approaching $4m^2$. This gives a spike of the same $(1-y)^{-1}$ shape as the two and three quantum annihilation spectrum with its radiative corrections,[3] but whose integrated contribution[13] is several orders of magnitude below the annihilation cross section. The phase-space integrals in this case are

$$\int A(p_2\leftrightarrow -p_3)d\Omega_4=\frac{8\pi}{3t^2}\left\{\left(z+\frac{1}{z}\right)\left(1+\frac{1}{x}\right)+\frac{t^2}{4k\cdot p_1}\left[\left(1+\frac{1}{z}\right)\left(4+\frac{9}{x}+\frac{2}{x^2}\right)+\frac{1}{xz}\left(\frac{4}{x}-2\right)\right]+\frac{t^4}{8(k\cdot p_1)^2}\left[\left(1+\frac{1}{z^2}\right)\left(\frac{1}{x^4}-\frac{9}{2x^3}-\frac{3}{x^2}-\frac{2}{x}\right)+\frac{1}{z}\left(4+\frac{2}{x}+\frac{3}{x^2}-\frac{11}{x^3}+\frac{2}{x^4}\right)\right]\right\}, \quad (13)$$

[12] L. I. Schiff, Phys. Rev. 83, 252 (1951).

[13] For a previous derivation of the integrated contribution, see U. Mosco, Nuovo Cimento 33, 115 (1964) and G. Longhi, *ibid.* 35, 1122 (1965).

TABLE IV. Additional parameters for each of the photon laboratory angles $\chi$ of Table III (first part). The lowest order annihilation cross section $d\sigma/d\Omega(e^+ + e^- \to 2\gamma)$ is given in mb/sr in the laboratory for an incident positron energy of 15 BeV (the corresponding c.m. energy is 126 MeV). Radiative corrections depend on the experimental resolution and so are omitted. The monochromatic photon energy $\omega_\gamma$ is essentially equal to $\omega_{\max}$ for the bremsstrahlung process. The corresponding center-of-mass angle is $\chi_{c.m.}$ and $z = k\cdot p_2/k\cdot p_1$ is a convenient dimensionless parameter to express the angular dependence in the wide-angle range.

| $\chi$ (rad) | $\omega_\gamma$ (BeV) | $d\sigma/d\Omega$ (mb/sr) | $\chi_{c.m.}$ (rad) | $z$ |
|---|---|---|---|---|
| 0.002 | 14.17 | 605.0 | 0.475 | 0.059 |
| 0.003 | 13.25 | 239.0 | 0.697 | 0.132 |
| 0.005 | 10.97 | 65.7 | 1.09 | 0.367 |
| 0.008 | 7.734 | 21.2 | 1.54 | 0.939 |
| 0.012 | 4.820 | 10.6 | 1.94 | 2.11 |

where $z = k\cdot p_2/k\cdot p_1$ and $x = t^2/2m^2$. Near the tip, the bremsstrahlung spectrum is well approximated by

$$\frac{d^2\sigma}{d\omega d\Omega} \approx \frac{\alpha r_0^2 m^2 \omega \beta}{3\pi (p_1\cdot p_2)}\left(1+\frac{2m^2}{t^2}\right)\left[\frac{1}{t^2}\left(z+\frac{1}{z}\right) + \frac{(\frac{1}{2}t^2 + t\cdot k)}{(k\cdot p_1)(k\cdot p_2)}\right]. \quad (14)$$

## ACKNOWLEDGMENTS

I wish to thank Dr. Y. S. Tsai, who originally suggested this problem as an application for my trace program, for valuable comment and criticism during the course of the work. My former advisor, Dr. C. K. Iddings, supervised the development of the trace program and the work with the numerical integration, and also gave considerable assistance with parts of the earlier manuscript drafts. Dr. A. Dufner, who used several of my numerical programs in compiling the tables of Ref. 6, is responsible for the general form of the numerical fit factor and for asking why the exact spectrum values seemed to go unbounded near the tip—a query which led to the verification of the contribution of the annihilation graphs in that region and indirectly to the modification of the trace program which produced Table I. I also thank Mr. C. H. Moore for help in the initial stages of the numerical work.

## APPENDIX

The historical development of this work has been in the reverse of logical order as refinements were added to surmount various difficulties which appeared. It had been originally hoped that we could simply grind out numerical integrals of the traces produced by the computer program, giving numerical values for the photon spectrum in the regions where the small-angle approximations were not expected to hold. This was frustrated by truncation errors and the extreme variation of the integrand which caused poor numerical and temporal convergence of the integrals until parts of the calculation were done in double precision and a change of variables devised which smoothed out the integrand. The first expressions for the basic traces of $\Sigma|M|^2$ remained an unintelligible jumble of terms until the capacity of the trace program was increased to allow substitutions of linear combinations of terms for invariants. Then the traces could be reduced to functions of a minimal set of invariants, and after considerable juggling, in which guesses for simplified forms were subtracted from the traces and then refined by analyzing the residue, the expressions of Table I were produced. The substitutional symmetries of the traces helped to suggest which variables and forms to use for the guesses. It is a simple matter to produce arithmetic expressions automatically from the output of the trace program which are then acceptable compiler input for subsequent numerical calculations.

A computer is ideally suited for the bookkeeping involved in the analytic evaluation of matrix elements. One might therefore expect that it could be used to evaluate many high-order quantities in quantum electrodynamics. Aside from the inordinate complexity of the intermediate results, one further trouble is that we have no algorithms for handling graphs with multiple, closed, internal loops. Such graphs, even if they are first obtained analytically, will probably have to be evaluated numerically. Thus the following discussion of the details of our numerical work may have some general interest if the singularities encountered in the general graphs are similar to those in our problem, and it will of particular interest to anyone who might wish to compute other points in the bremsstrahlung spectrum.

There are two principal sources of computational errors: (1) The numbers are represented by finite strings of digits; if the final answer is the result of a near cancellation of several terms, there can be appreciable truncation error. (2) A numerical integration of a rapidly varying function such as $\Sigma|M|^2$ may be inaccurate because the mesh points miss important regions of variation of the integrand.

We have estimated the errors of type (1) by calculating $\Sigma|M|^2$ at various points ($\theta$, $\phi$ in special frame) in double precision and comparing this to $\Sigma|M|^2$ calculated at the same point, but in single precision.[14] Our conclusion is that the "single-precision" calculation gives at least one or two significant decimal digits in the worst case (in the depressions near the center of the peaks, in regions contributing about 8% to the total integral), and that the round-off and truncation errors in the final answers are less than 0.1%.

The final-state integration was initially attempted with respect to $d(\cos\theta)d\phi$, using a recursive Simpson's

[14] Double precision is about 23 decimal digits on the Burroughs B-5500. Actually, in our "single-precision" calculation the dot products of Table II and the photon propagators were evaluated in double precision and then truncated to single precision. The $\Sigma|M|^2$ and subsequent numerical integration was then done in single precision.

rule. This algorithm refined the mesh in regions of rapid variation of the integrand until a specified agreement was obtained between two successive approximations.[15] Blind application of this routine gave very poor accuracy; apparently, sometimes one of the peaks was completely missed. By requiring that the initial trial mesh contain several points in the vicinity of each maximum, we obtained more accurate answers, but excessive computation time was needed to get better than 10% accuracy for small-angle, small-photon-energy points. At such points, the convergence of our integral routine was not completely satisfactory because of the extreme variation of $\Sigma|M|^2$ near a maximum. It was suggested to us that by a transformation of variables, equal intervals of integration could be made to have approximately equal contributions to the final answer.[16] In other words, by introducing a variable change of scale, the integrand can be made much smoother and better convergence results. In principle, the recursive mesh refinement also spends approximately equal times sampling the integrand in regions of equal contribution to the integral; it turned out to be less efficient in practice under conditions of extreme variation. The numerical answers obtained by using this change of variables are estimated to be accurate to 1% except for a few points at small $x$ and small $y$ (these points are marked by an asterisk in Table III, and are probably 3–6% low). This estimate of accuracy is based on a comparison of the numerical and analytic integrals of the part of $\Sigma|M|^2$ used in the approximations discussed in the article (column **5**). Since this truncated integrand closely resembles the exact expression, we assume that the exact integral is also accurate to 1% when the comparison on the truncated integrals shows this accuracy.

We now indicate the exact nature of the change of variables used to smooth out the integrand. Bear in mind that the integrand is approximately proportional to an appropriate $q^{-2}$ near a peak. For the electron propagators, $k\cdot p_3$ and $k\cdot p_4$, the maxima occur at $\theta=0$, $\pi$ and the integrand is approximately constant in $\phi$. The substitution is

$$q^2=a\pm b\cos\theta=be^u, \tag{15}$$

$$bd(\cos\theta)d\phi=\pm q^2dud\phi. \tag{16}$$

In the photon propagators, the peak is associated with $\phi=0$, and

$$\cos\theta_1=-(t\cdot p_1-t^2k\cdot p_1/t\cdot k)[(t\cdot p_1)^2-m^2t^2]^{-1/2}, \tag{17}$$

or

$$\cos\theta_2=(t\cdot p_2-t^2k\cdot p_2/t\cdot k)[(t\cdot p_2)^2-m^2t^2]^{-1/2}. \tag{18}$$

We put

$$q^2=a-b(\cos\theta_i\cos\theta+\sin\theta_i\sin\theta\cos\phi)=a'-b'\cos\phi, \tag{19}$$

$$\tan\tfrac{1}{2}\phi=(a'-b')^{1/2}(a'+b')^{-1/2}\tan v, \tag{20}$$

$$\tan\tfrac{1}{2}(\theta-\theta_i)=(a-b)^{1/2}(a+b)^{-1/2}\sinh u, \tag{21}$$

$$d(\cos\theta)d\phi=-4q^2(a+b)^{-1/2}(a'+b')^{-1/2}\times\sin\theta\cos\tfrac{1}{2}(\theta-\theta_i)dvdu. \tag{22}$$

The integration was done by iteration of single integrals, with $\int d\phi$ or $\int dv$ performed first. Note that since the integrand depends only on

$$\cos\phi, \quad \int_0^{2\pi}d\phi=2\int_0^{\pi}d\phi.$$

Because of the difficulty in obtaining convergent, accurate numerical integrals, our conclusion is that any computer evaluation of complicated matrix elements cannot ignore physical insights about possible singularities. In particular, a program designed to evaluate any arbitrary (lowest order) process is feasible,[17] but if it is to be useful over the range of energies presently available experimentally, it will probably have to perform arithmetical operations in double precision and include some means of locating and treating carefully the near zeros of propagator denominators. Perhaps bremsstrahlung is a hard test case, since photon propagators are generally much more singular than electron propagators.

[15] We are indebted to C. H. Moore, formerly of the SLAC Computation Group, for this algorithm.

[16] E. A. Allton (private communication).

[17] Large steps toward the development of such a program have been made at Stanford in the list processing language LISP 1.5: A. C. Hearn, Bull. Am. Phys. Soc. **9**, 436 (1964); Commun. ACM **9**, 573 (1966).